Modeling the next battery generation: Lithium-sulfur and lithium-air cells

D. N. Fronczek, T. Danner, B. Horstmann, Wolfgang G. Bessler
German Aerospace Center (DLR)
University Stuttgart (ITW)
Helmholtz Institute Ulm for Electrochemical Energy Storage (HIU)

wolfgang.bessler@dlr.de
www.bessler.info

Deutsches Zentrum für Luft- und Raumfahrt e.V. in der Helmholtz-Gemeinschaft
HIU
HELMHOLTZ GEMEINSCHAFT
Bundesministerium für Bildung und Forschung

Research profile: Computational battery technology

Lithium-ion technology

$LiFePO_4$ batteries: Electrochemistry and impedance

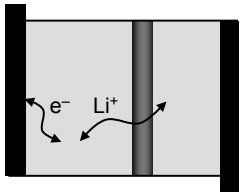

Understanding and optimization of physicochemical behavior

Thermal management and runaway risk

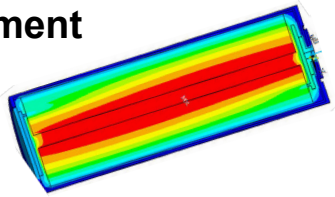

Understanding and optimization of thermal and safety behavior

Post-lithium-ion cells

Lithium-sulfur cells: Redox chemistry and transport

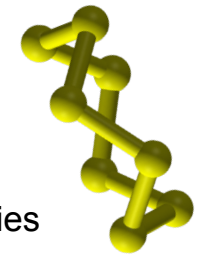

Analysis of cycling properties and chemical reversibility

Lithium-air cells: Multi-phase chemistry and reversibility

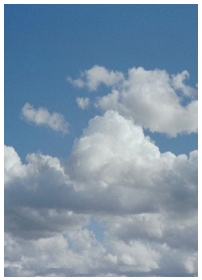

Improvement of porous air electrode

Multi-scale and multi-physics modeling and numerical simulation

Motivation and approach

Lithium-sulfur

Lithium-air (organic)

Lithium-air (aqueous)

Conclusions

Motivation and approach

Lithium-sulfur

Lithium-air (organic)

Lithium-air (aqueous)

Conclusions

Li-S and Li-O: Challenges

- Complex multi-phase management
  - Li-S: Solid reactant S_8 and product Li_2S, solid precipitates
  - Li-O: Solid, liquid and gas phase involved
- Complex chemistry
  - Li-S: Polysulfide ion intermediates
  - Li-O: Oxygen reduction as traditional problem of electrochemistry
- Low cycleability, low efficiency
- **Computational modeling for understanding and optimization**

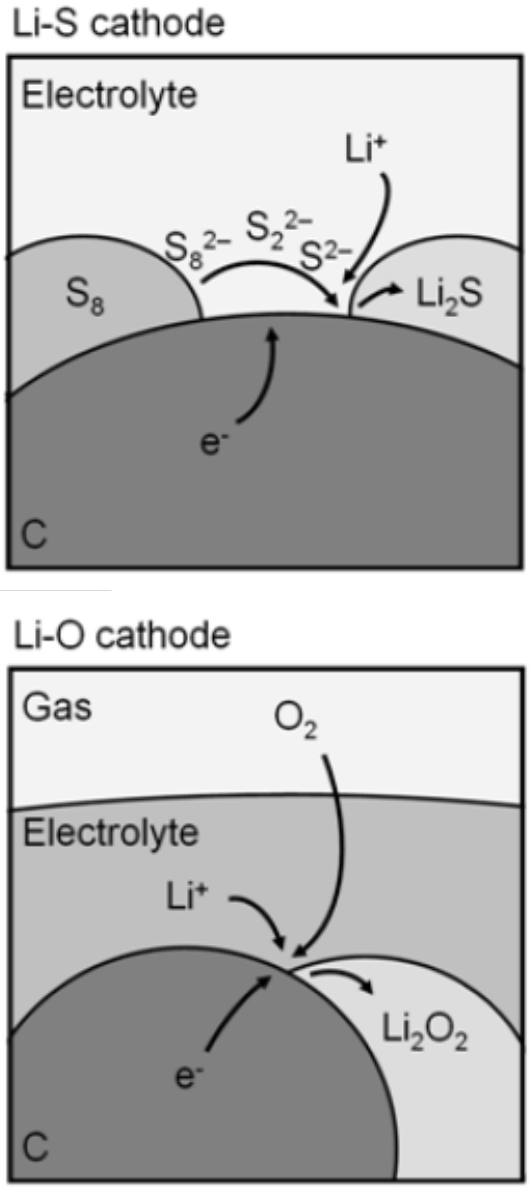

1D/2D generic modeling framework

- Electrochemical cell of up to seven **layers**
- Each layer consists of arbitrary number of solid, liquid and/or gaseous **bulk phases**
- Each layer can contain an arbitrary number of **interfaces** (phase boundaries)
- Each bulk phase consists of arbitrary number of **chemical species**
- **Chemistry** takes place at interfaces
- **Transport** mechanisms (liquid, solid, gas)
- **Continuum** (homogenization) approach

J. P. Neidhardt, D. N. Fronczek, T. Jahnke, T. Danner, B. Horstmann and W. G. Bessler, J. Electrochem. Soc., submitted (2012).

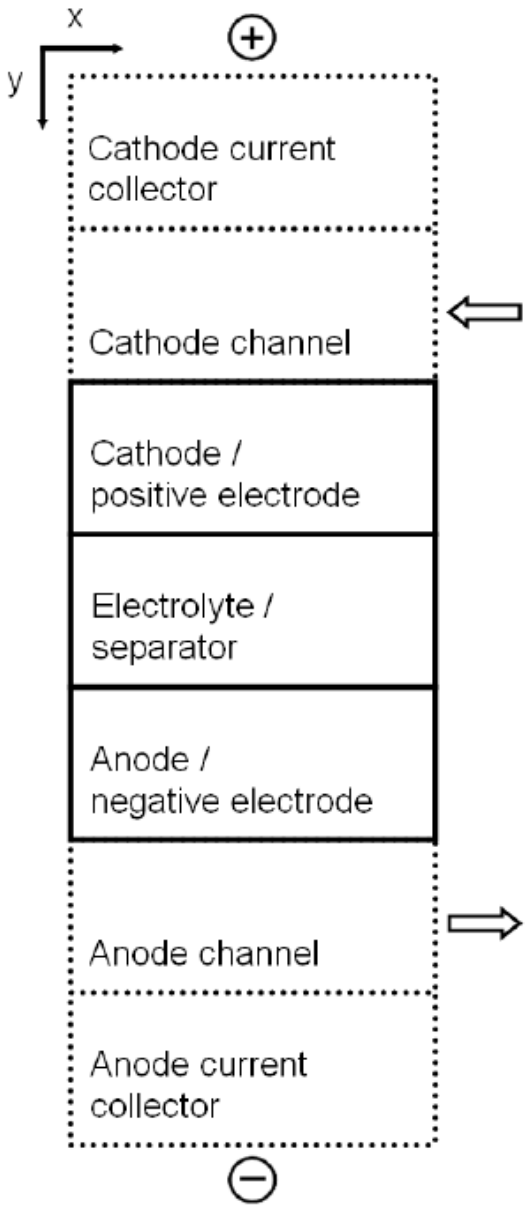

Chemical reactions at interfaces

- Mass-action kinetics describes chemical source terms $\dot{s}_i$

$$\dot{s}_i = \nu_i \left(k_f \prod_{j \in R_f} c_j^{\nu_j'} - k_r \prod_{j \in R_r} c_j^{\nu_j''} \right)$$

ν stoichiometric coefficient
k reaction rate constant
c concentration of reactants

- Rate constants described by modified Arrhenius expression. Reverse rate follows from thermodynamic consistency.

$$k_f = A^{\mathrm{f}} T^{\beta} \exp\left(-\frac{E^{\mathrm{act}}}{RT}\right) \exp\left(-\frac{\alpha z F}{RT} \Delta\phi\right) \qquad \frac{k_f}{k_r} = \exp\left(-\frac{\Delta G^0}{RT}\right)$$

Preexponential factor

Temperature dependence (Activation energy E^{act})

Potential dependence (Half-cell potential $\Delta\phi$)

Multi-phase management

- The volume fraction ε_i of each phase *i* depends on time

$$\frac{\partial(\varepsilon_i \rho_i)}{\partial t} = R_i M_i$$

ε volume fraction
ρ density
R chemical formation rate
M molar mass

- Volume fractions sum up to one. Def. of compressible phase necessary.

$$\sum \varepsilon_i = 1$$

- Microstructural effects enter via interfacial area and transport coefficients

$$A^{\mathrm{V}}_{m,n} = A^{\mathrm{V}}_0 \cdot f(\varepsilon_m, \varepsilon_n)$$

A^V volume-specific surface area / m^2/m^3

$$D_i^{\mathrm{eff}} = \frac{\varepsilon_i}{\tau_i^2} D_i \qquad \sigma_i^{\mathrm{eff}} = \frac{\varepsilon_i}{\tau_i^2} \sigma_i$$

D diffusion coefficient
σ Conductivity

Mass and charge transport in liquid electrolyte

- Species conservation (Nernst-Planck equation)

$$\frac{\partial(\varepsilon c_i)}{\partial t} = -\frac{\partial J_i}{\partial y} + \sum_m A_m^{\mathrm{V}} \dot{s}_{i,m}$$

$$J_i = -D_i^{\mathrm{eff}} \frac{\partial c_i}{\partial y} - D_i^{\mathrm{migr,eff}} \frac{\partial \phi_{\mathrm{elyt}}}{\partial y}$$

- Charge neutrality

$$0 = -\sum_i z_i F \frac{\partial J_i}{\partial y} + \sum_m z_i F \, A_m^{\mathrm{V}} \dot{s}_{i,m}$$

- Diluted solution theory (Li-S)

$$D_i^{\mathrm{migr}} = \frac{z_i F}{RT} c_i D_i$$

- Concentrated solution theory (Li-O)

$$D_{\pm} = D^0 + \frac{t_{\pm}}{z_+ F} \frac{\sigma_D}{c_{\pm}}$$

$$D_{\pm}^{\mathrm{migr}} = \frac{t_{\pm}}{z_{\pm} F} \sigma$$

DLR HIU

Multi-scale simulation framework

- DENIS: Detailed Electro-chemistry and Numerical Impedance Simulation
- In-house C/C++ software
- Workhorse of the group

m

nm

System

Stack

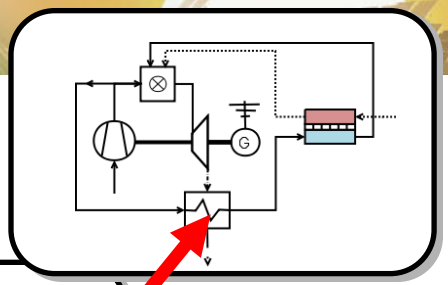

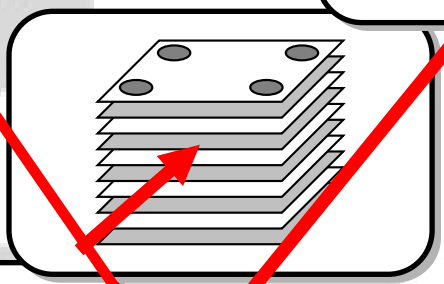

MATLAB

Coupling DENIS-SIMULINK

Cell

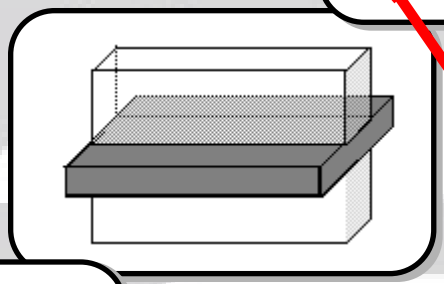

DENIS

ANSYS/COMSOL

Coupling DENIS-ANSYS/COMSOL for CFD simulations

Electrode

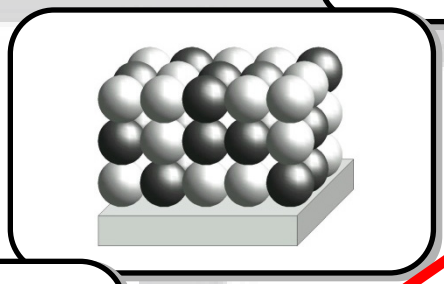

LIMEX

Implicit DAE solver (Deuflhard, Berlin)

Interfaces

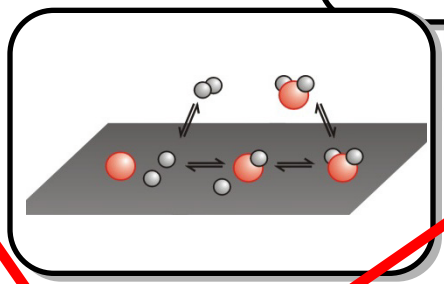

CANTERA

Coupling with CANTERA (Goodwin, Caltech) for chemistry source terms and transport coefficients

Motivation and approach

Lithium-sulfur

Lithium-air (organic)

Lithium-air (aqueous)

Conclusions

Li-S battery modeling domain

Cathode properties:

- Thickness: 41 µm
- Phases (charged state):
  - Sulfur $\varepsilon = 0.16$
  - Carbon $\varepsilon = 0.06$
  - Electrolyte $\varepsilon = 0.78$
  - Li_2S $\varepsilon = 10^{-7}$
- Interfaces:
  - Sulfur-Electrolyte
  - Carbon-Electrolyte
  - Li_2S-Electrolyte

Anode: Lithium metal

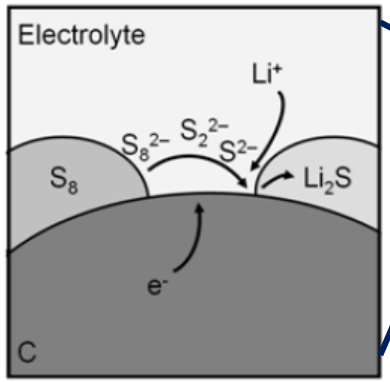

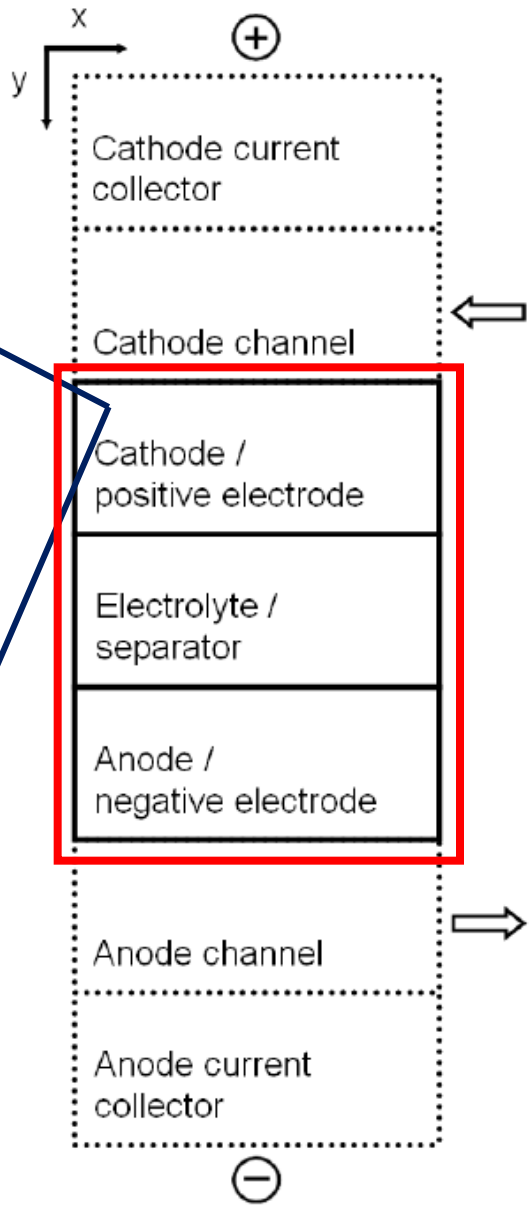

Li-S battery model: Thermodynamics and transport

Species	Molar Gibbs energy / $kJ \cdot mol^{-1}$	Density / Initial concentration	Diffusion coefficient / $m^2 \cdot s^{-1}$
Li	0	$5.34 \cdot 10^2\ kg \cdot m^{-3}$	
C	0	$2.26 \cdot 10^3\ kg \cdot m^{-3}$	
$S_8^{(solid)}$	0	$2.07 \cdot 10^3\ kg \cdot m^{-3}$	
Li_2S	−441.4		
$C_4H_6O_3$	0	$9.831 \cdot 10^3\ mol \cdot m^{-3}$	
Li^+	0	$9.841 \cdot 10^2\ mol \cdot m^{-3}$	$1 \cdot 10^{-10}$
PF_6^-	0	$9.830 \cdot 10^2\ mol \cdot m^{-3}$	$4 \cdot 10^{-10}$
S^{2-}	−405.08	$8.127 \cdot 10^{-10}\ mol \cdot m^{-3}$	$1 \cdot 10^{-10}$
S_2^{2-}	−422.29	$5.141 \cdot 10^{-7}\ mol \cdot m^{-3}$	$1 \cdot 10^{-10}$
S_4^{2-}	−450.91	$1.966 \cdot 10^{-2}\ mol \cdot m^{-3}$	$1 \cdot 10^{-10}$
S_6^{2-}	−460.23	$3.185 \cdot 10^{-1}\ mol \cdot m^{-3}$	$6 \cdot 10^{-10}$
S_8^{2-}	−461.20	$1.750 \cdot 10^{-1}\ mol \cdot m^{-3}$	$6 \cdot 10^{-10}$
$S_8^{(liquid)}$	−48	$1.868\ mol \cdot m^{-3}$	$1 \cdot 10^{-9}$

- Parameters converted from Kumaresan et al., J. Electrochem. Soc. 155, A576 (2008)

DLR HIU

Li-S battery model: Reactions and kinetics

Reaction	Preexponential factor, forward reaction	Preexponential factor, reverse reaction
$Li \rightleftarrows Li^+ + e^-$	$4.086 \cdot 10^{-9}$ $m^{-5} \cdot mol^2 \cdot s^{-1}$	1 $m^{-2} \cdot mol \cdot s^{-1}$
$S_8^{(solid)} \rightleftarrows S_8^{(liquid)}$	$1.900 \cdot 10^{-2}$ $m^{-0.5} \cdot mol^{0.5} \cdot s^{-1}$	1 s^{-1}
$\frac{1}{2} S_8^{(solid)} + e^- \rightleftarrows \frac{1}{2} S_8^{2-}$	$7.725 \cdot 10^{13}$ $m^{-0.5} \cdot mol^{0.5} \cdot s^{-1}$	$2.940 \cdot 10^{-27}$ $m^{-0.5} \cdot mol^{0.5} \cdot s^{-1}$
$\frac{3}{2} S_8^{2-} + e^- \rightleftarrows 2\, S_6^{2-}$	$4.331 \cdot 10^{16}$ $m \cdot mol^{-0.5} \cdot s^{-1}$	$1.190 \cdot 10^{-23}$ $m^4 \cdot mol^{-1} \cdot s^{-1}$
$S_6^{2-} + e^- \rightleftarrows \frac{3}{2} S_4^{2-}$	$3.193 \cdot 10^{14}$ s^{-1}	$4.191 \cdot 10^{-24}$ $m \cdot mol^{-0.5} \cdot s^{-1}$
$\frac{1}{2} S_4^{2-} + e^- \rightleftarrows S_2^{2-}$	$2.375 \cdot 10^{11}$ $m^{-0.5} \cdot mol^{0.5} \cdot s^{-1}$	$7.505 \cdot 10^{-24}$ s^{-1}
$\frac{1}{2} S_2^{2-} + e^- \rightleftarrows S^{2-}$	$4.655 \cdot 10^{12}$ $m^{-0.5} \cdot mol^{0.5} \cdot s^{-1}$	$4.738 \cdot 10^{-22}$ s^{-1}
$2\, Li^+ + S^{2-} \rightleftarrows Li_2S^{(solid)}$	$2.750 \cdot 10^{-5}$ $m^6 \cdot mol^2 \cdot s^{-1}$	$8.250 \cdot 10^{-19}$ s^{-1}

- Parameters converted from Kumaresan et al., J. Electrochem. Soc. 155, A576 (2008)

Li-S: Simulated discharge curve and phase change

- Discharge shows typical two-stage behavior
- Solid S_8 is fully consumed before solid Li_2S is formed

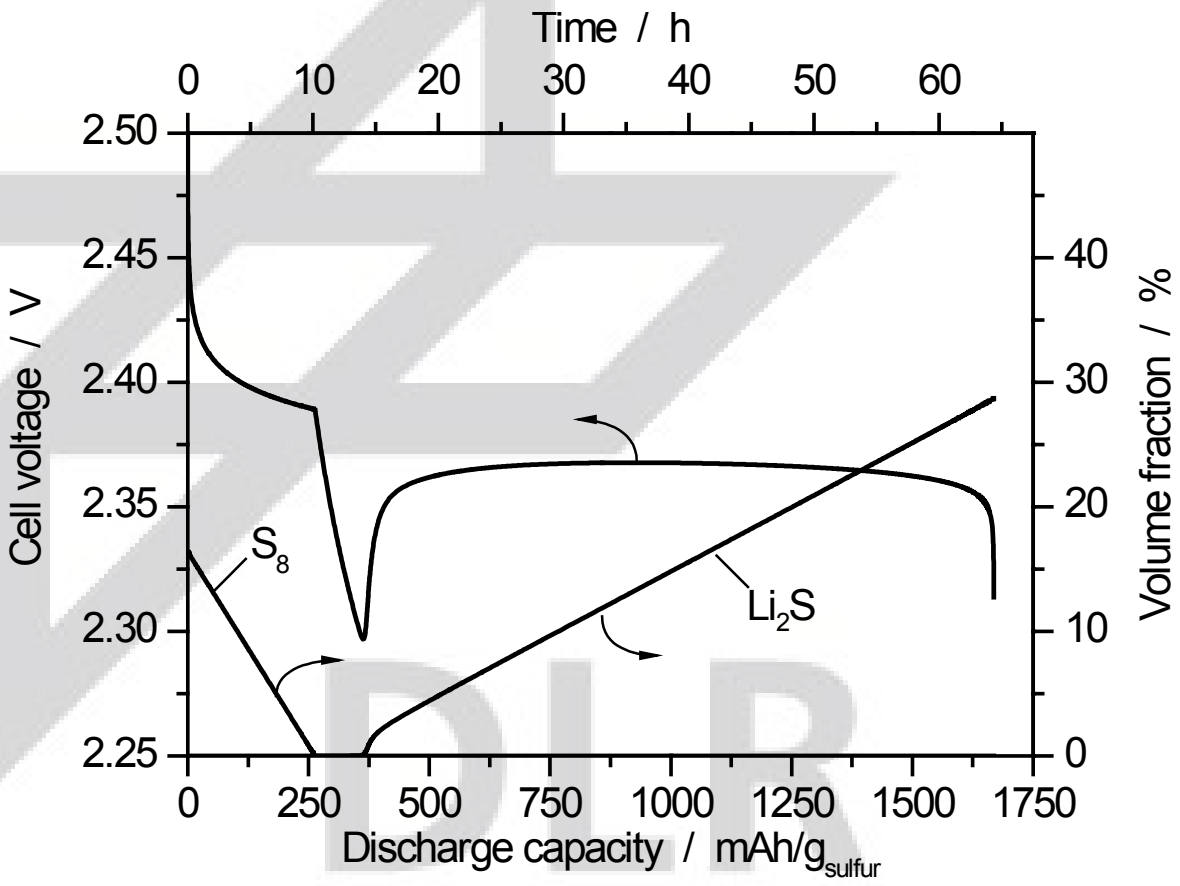

Li-S: Simulated ionic species concentrations

- First stage: Sulfur polyanions are formed
- Second stage: Sulfur polyanions are reduced
- End of discharge: No more sulfur polyanions

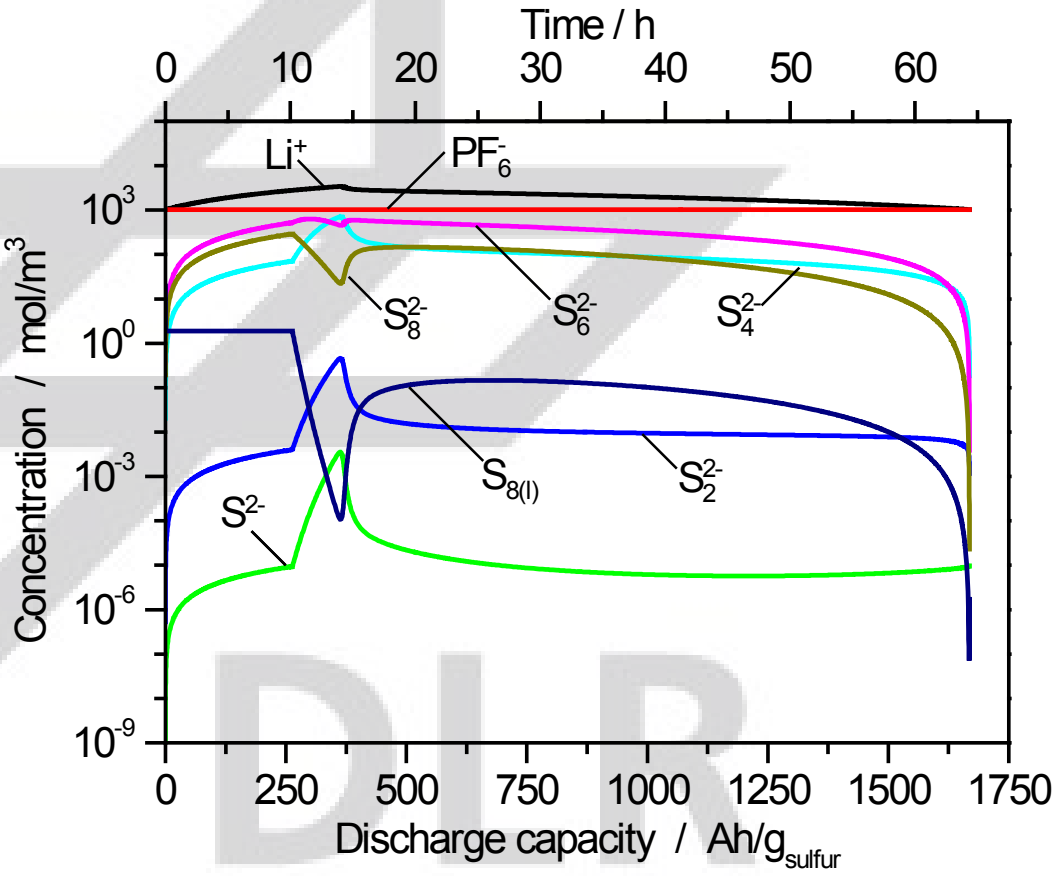

Motivation and approach

Lithium-sulfur

Lithium-air (organic)

Lithium-air (aqueous)

Conclusions

Li-O battery modeling domain

Cathode properties:

- Thickness: 750 µm
- Phases:
  - Carbon $\varepsilon = 0.25$
  - Electrolyte $\varepsilon = 0.75$
  - Li_2O_2 $\varepsilon = 10^{-7}$
- Interfaces:
  - Carbon-Electrolyte-Li_2O_2

Electrolyte: $LiPF_6$ / Stable organic solvent

Anode: Metallic lithium

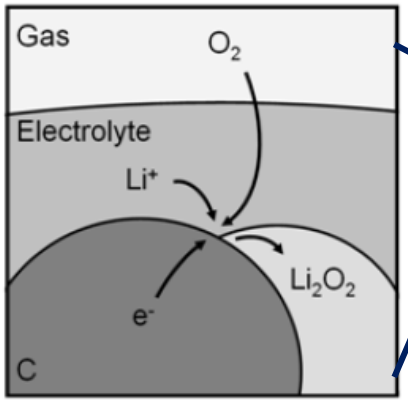

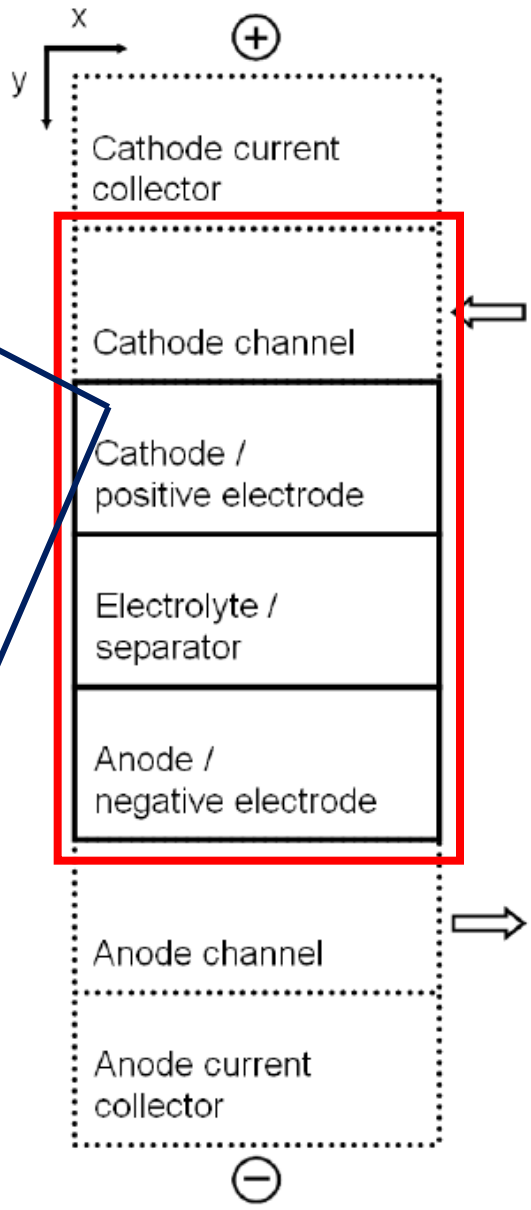

Li-O battery model: Thermodynamics and kinetics

Species	Molar Gibbs energy / $kJ \cdot mol^{-1}$	Density / Initial concentration
Li	0	$5.34 \cdot 10^{2}\ kg \cdot m^{-3}$
Li^{+}	0	$1.0 \cdot 10^{3}\ mol \cdot m^{-3}$
PF_6^{-}	–	$1.0 \cdot 10^{3}\ mol \cdot m^{-3}$
$O_2^{(gas)}$	−61	21 %
$O_2^{(dissolved)}$	−43	$1.62\ mol \cdot m^{-3}$
Li_2O_2	−644	$2.14 \cdot 10^{3}\ kg \cdot m^{-3}$
EC-EMC	–	$1.07 \cdot 10^{4}\ mol \cdot m^{-3}$

Reaction	Preexponential factor, forward reaction	Activation energy
$Li \rightleftarrows Li^{+} + e^{-}$	$1.31 \cdot 10^{-1}\ m \cdot s^{-1}$	0
$O_2^{(gas)} \rightleftarrows O_2^{(dissolved)}$	Assumed in equilibrium	–
$2\ Li^{+} + O_2^{(dissolved)} + 2\ e^{-} \rightleftarrows Li_2O_2$	$9.23 \cdot 10^{31}\ m^{7} \cdot mol^{-2} \cdot s^{-1}$	0

- Parameters converted from: P. Andrei, J. P. Zheng, M. Hendrickson and E. J. Plichta, J. Electrochem. Soc., 157, A1287 (2010); A. Nyman, M. Behm and G. Lindbergh, Electrochim. Acta, 53, 6356 (2008); R. C. Weast, Handbook of chemistry and physics, CRC Press (1982).

Li-O: Simulated discharge behavior

- Discharge curves simulated for different current densities
- Polarization losses increase with increasing current density
- Capacity strongly depends on current density

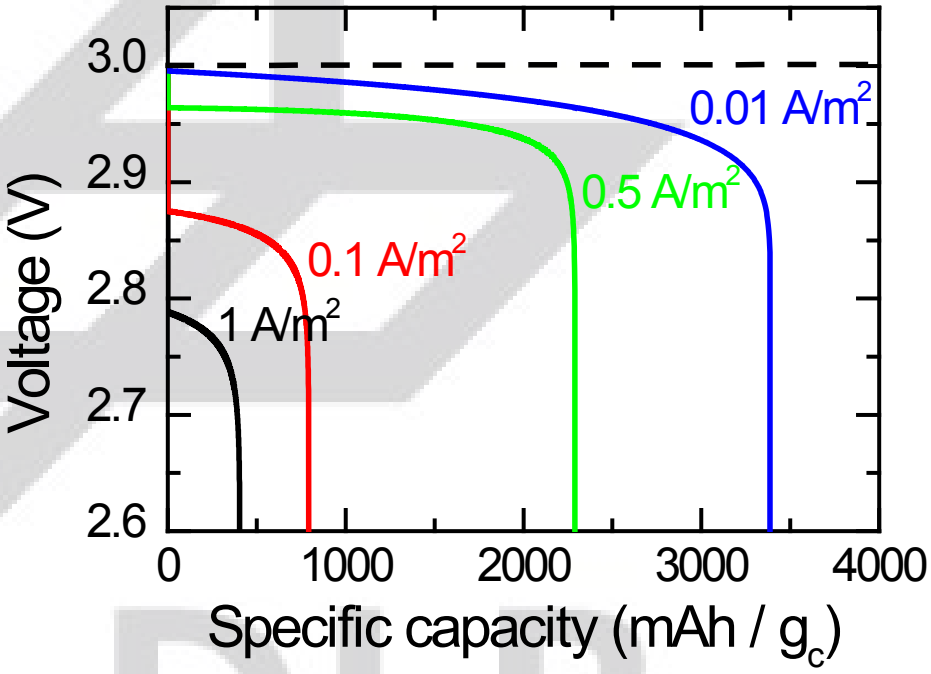

Li-O: Spatial distribution

- Strong gradients of dissolved O_2 in organic electrolyte
- At high currents, reactions are confined to regions close to channel
- **Rate-limiting O_2 diffusion is origin of polarization losses**

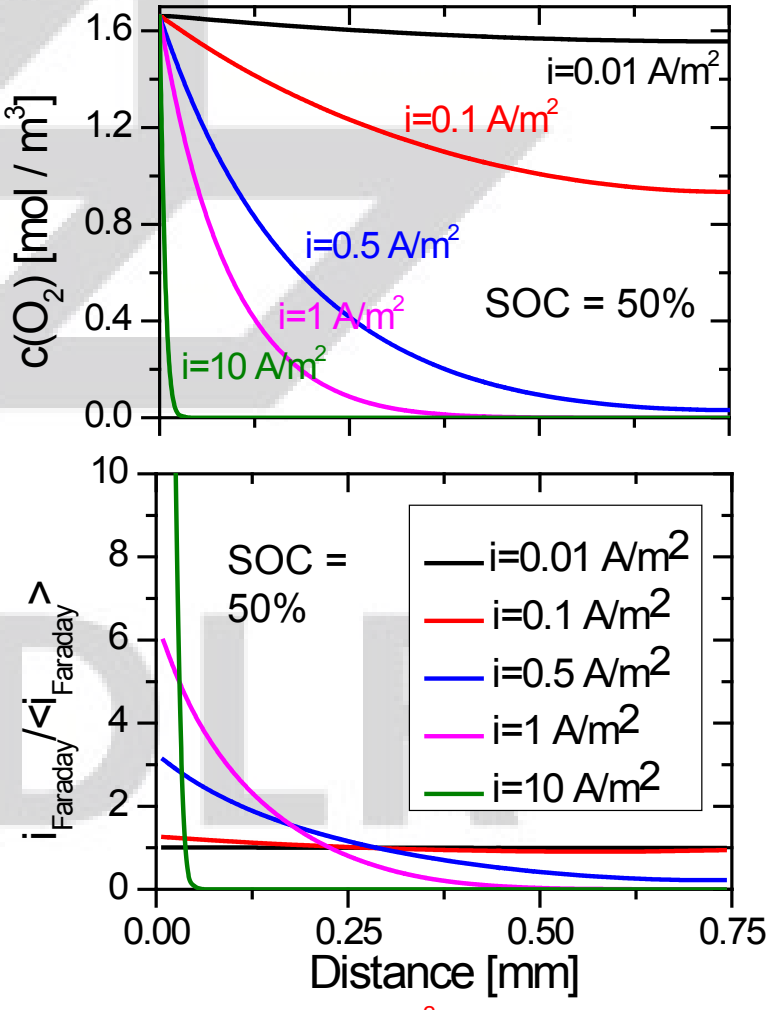

Li-O: Pore clogging

- Free porosity decreases upon discharge
- Pore clogging by product Li_2O_2
- Clogging stronger close to channel
- Strong gradients for high currents
- **Pore clogging is origin of current-dependent capacity loss**

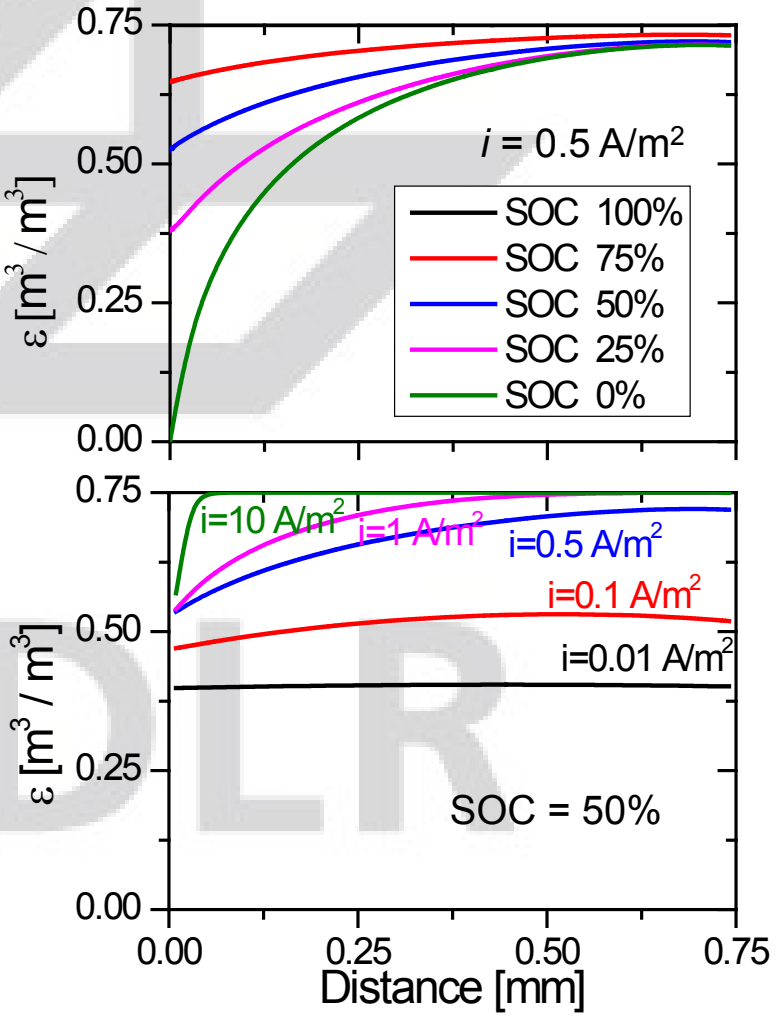

Motivation and approach

Lithium-sulfur

Lithium-air (organic)

Lithium-air (aqueous)

Conclusions

Aqueous Li-O: LiOH as soluble intermediate

- Oxygen reduction:
  $O_2 + 4\ e^- + 2\ H_2O \rightleftarrows 4\ OH^-(aq)$
- Precipitation:
  $Li^+ + OH^- + H_2O \rightleftarrows LiOH \cdot H_2O(s)$

Aqueous Li-O modeling domain

Cathode properties:

- Thickness: 500 µm
- Phases (start composition):
  - Carbon $\varepsilon = 0.25$
  - Water $\varepsilon = 0.75$
  - $LiOH \cdot H_2O$ $\varepsilon = 10^{-7}$
- Interfaces:
  - Carbon-Electrolyte-$LiOH \cdot H_2O$

Separator properties:

- Porous thickness: 100 µm
- Ideal separation from anode assumed (e.g., Li^+-conducting glass)

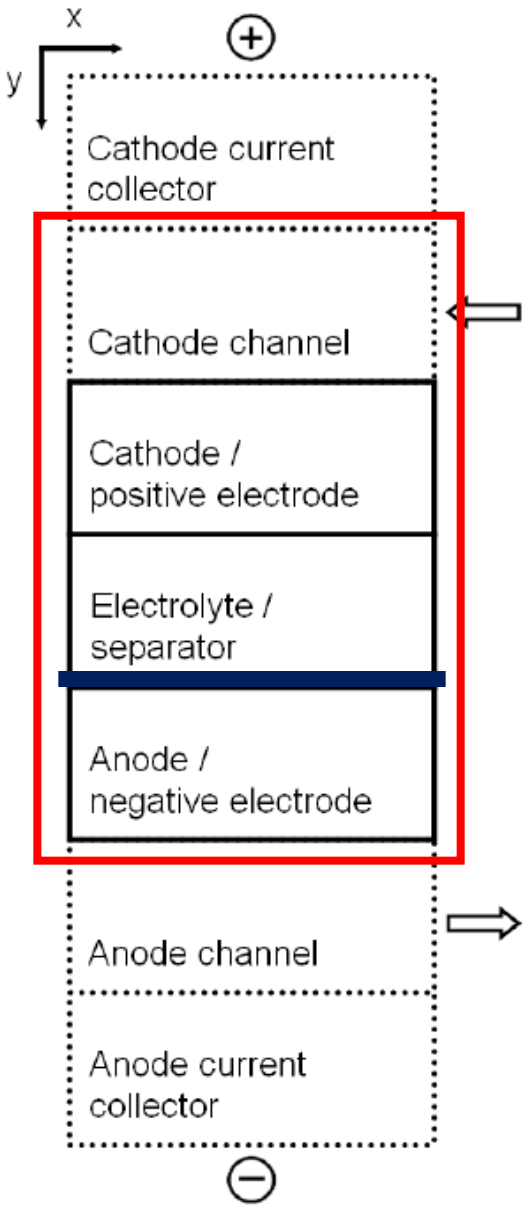

Results: Aqueous Li-O battery

- Two-stage discharge
- I: Dissolved LiOH
  Small voltage variation
- II: Precipitation of $LiOH \cdot H_2O$
  Constant voltage
- End of discharge:
  Capacity limited by LiOH precipitation

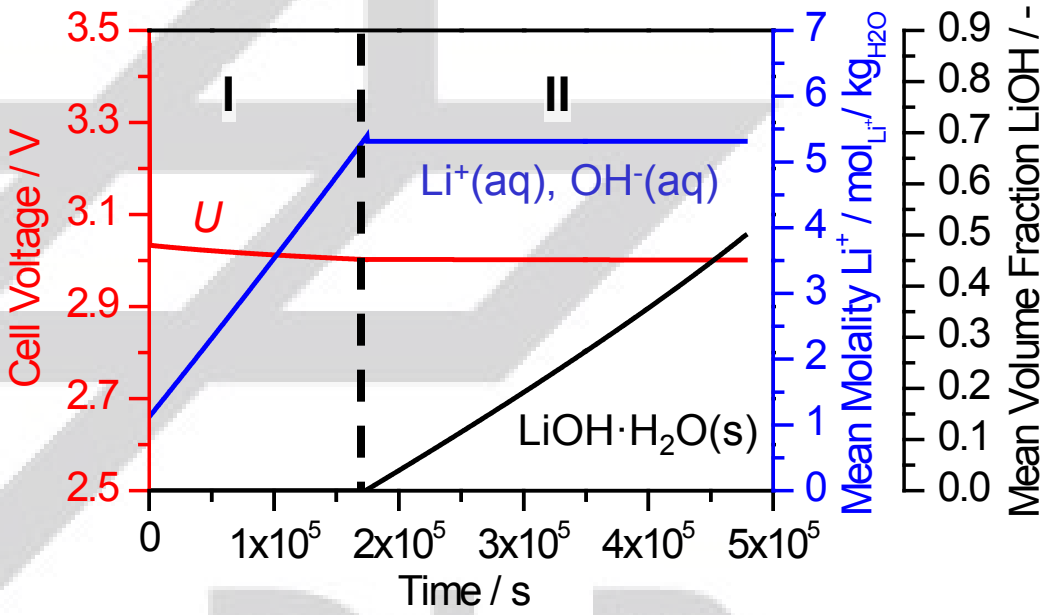

Concentration distribution

- A Li^+/OH^- concentration gradient, peak at anode
- B Increasing Li^+/OH^- concentration
- C Beginning LiOH precipitation within separator close to anode
- D LiOH precipitation at oxygen inlet and anode surface
- ➔ **End of discharge due to LiOH film on anode surface**

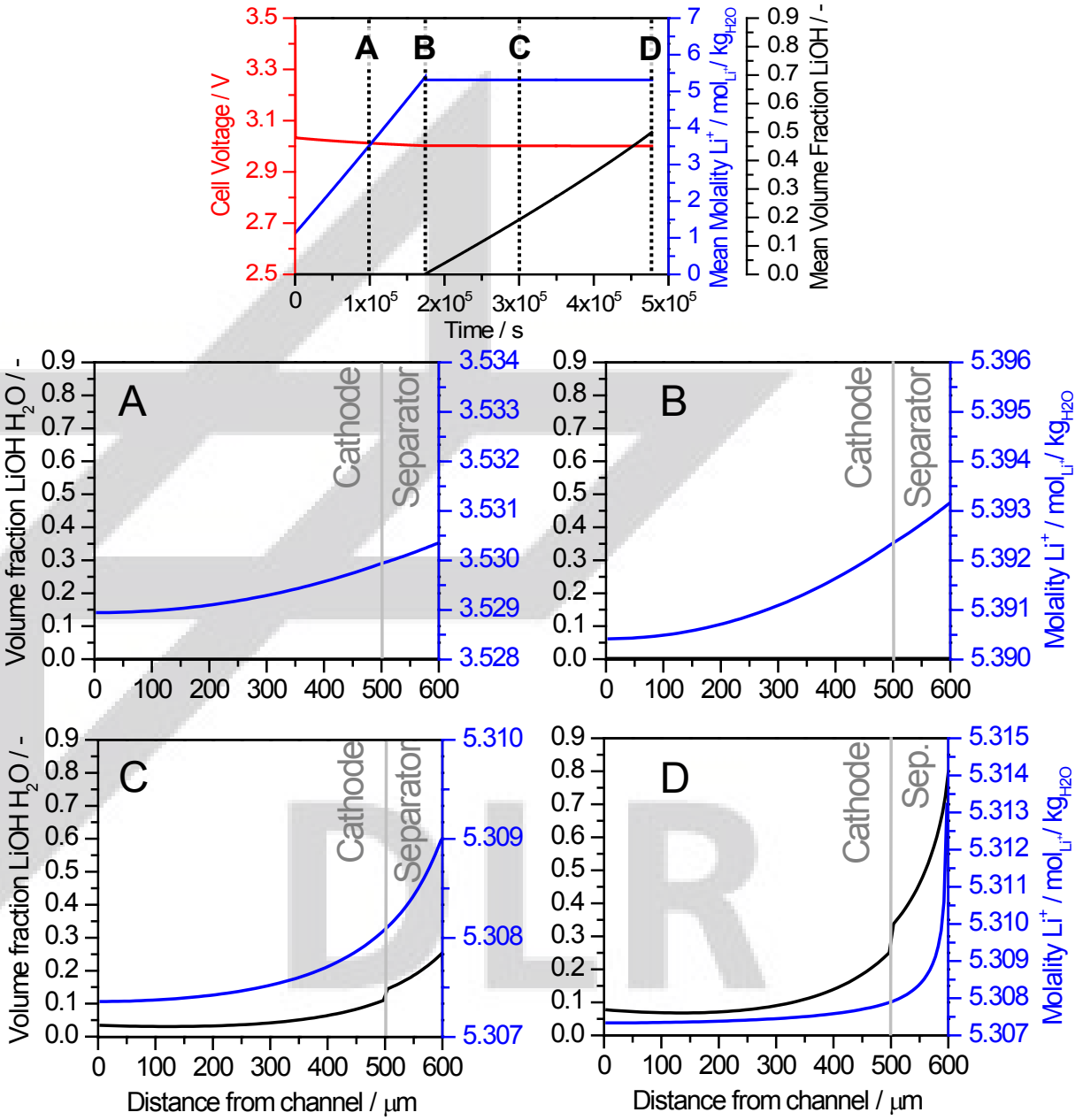

Motivation and approach

Lithium-sulfur

Lithium-air (organic)

Lithium-air (aqueous)

Conclusions

Summary: Next-generation battery modeling

- Li-S and Li-O batteries: High energy density, low cycleability
- Challenges: Complex chemistry and complex multi-phase behavior
- Chemistry, phases and transport included into modeling framework
- Li-S: Two-stage behavior: Dissolution, charge transfer, precipitation mechanism
- Li-O organic: Low oxygen diffusivity and pore clogging at channel
- Li-O aqueous: Low oxygen diffusivity and pore clogging at anode

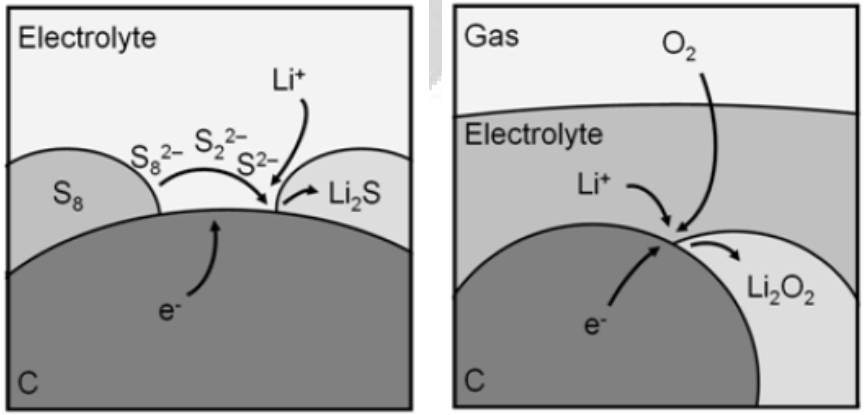

Thank you for your attention!

wolfgang.bessler@dlr.de · www.bessler.info